

Extracting the Odderon from pp and $p\bar{p}$ scattering data

András Ster*

*Wigner Research Centre for Physics, Hungarian Academy of Sciences,
H-1525 Budapest 114, P.O. Box 49, Hungary*

László Jenkovszky†

*BITP, National Academy of Sciences of Ukraine, Kiev, 03680 Ukraine and
Wigner Research Centre for Physics, Hungarian Academy of Sciences,
H-1525 Budapest 114, P.O. Box 49, Hungary*

Tamás Csörgő‡

*Wigner Research Centre for Physics, Hungarian Academy of Sciences,
H-1525 Budapest 114, P.O. Box 49, Hungary and
KRF, H-3200 Gyöngyös, Mátrai út 36, Hungary*

(Dated: June 16, 2021)

Abstract

Starting from a simple empirical parametrization of the scattering amplitude, successfully describing the dip-bump structure of elastic pp scattering in t at fixed values of s , we construct a toy model interpolating between missing energy intervals to extract the Odderon contribution from the difference between $\bar{p}p$ and pp elastic and total cross sections. The model is fitted to data from $\sqrt{s} = 23.5$ GeV to 7 TeV and used to extract the Odderon and its ratio to the Pomeron. From our fits, a unit intercept Odderon follows, as predicted by J. Bartels, L.N. Lipatov, and G.P. Vacca, on the basis of perturbative quantum chromodynamics.

PACS numbers: 13.75.Cs, 13.85.-t

Keywords: Elastic and total cross sections

* ster@rmki.kfki.hu

† jenk@bitp.kiev.ua

‡ csorgo.tamas@wigner.mta.hu

I. INTRODUCTION

The nature of the Odderon — an asymptotic odd- C Regge pole exchange, counterpart of the Pomeron — for a long time remains a subject of debate. Although there is little doubt about its existence, we still lack direct evidence of the Odderon. Various reactions supposedly dominated by Odderon exchanges, called “Odderon filters” [1], may offer only indirect evidence either because of low statistics or contamination by competing exchanges.

In quantum chromodynamics the Odderon corresponds to the exchange of an odd number of gluons. Relevant calculations were done in a number of papers; see [2] and earlier references therein.

The only direct way to see the Odderon is by comparing particle and antiparticle scattering at high enough energies. The high-energy proton-proton and proton-antiproton elastic scattering amplitude is a difference or sum of even and odd C -parity contributions, $A_{pp}^{\bar{p}p}(s, t) = \text{“Even”} \pm \text{“Odd”}$, where, essentially, the even part consists of the Pomeron and f Reggeon, while the odd part contains the Odderon and the ω Reggeon. It is clear from the above formula that the odd component of the amplitude can be extracted from the difference of the proton-antiproton and proton-proton scattering amplitudes, and, since at high enough energies the contributions from secondary Regge trajectories die out, this difference offers a direct way of extracting the Odderon contribution. Unfortunately, pp and $\bar{p}p$ elastic scatterings were typically measured at different \sqrt{s} , with the exception of the ISR energies of 31, 53, 62 GeV (see Fig. 1).

At present, the only way to extract the Odderon from the difference of the $\bar{p}p$ and pp scattering amplitudes is by means of a reliable interpolation of both amplitudes (or cross sections) over the missing energy regions. While the energy dependence of the forward amplitude (or total cross sections) is controlled by the Regge pole theory, its t dependence, especially in the dip-bump region, to a large extent is model dependent and unpredictable.

A simple, general, and reliable parametrization of the complicated diffraction structure at high energies at any fixed energy is a sum of two exponentials in t related by a complex phase $e^{i\phi}$. Using this generic expression, Phillips and Barger (PB) [3] (for brevity we shall refer to it as the PB ansatz) obtained good fits to the proton-proton differential cross sections, including the dip-bump region at several CERN ISR fixed energies. In Refs. [5–7] the model was extended and improved, in particular, by accounting for the nonexponential behavior

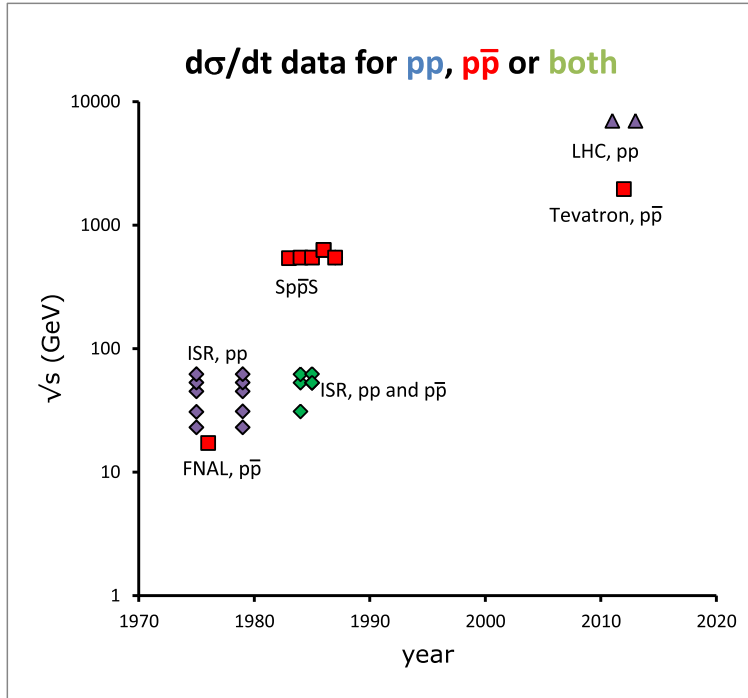


FIG. 1. Timeline of proton and antiproton elastic scattering measurements. New accelerators are run first at the maximum available energies; however, at the start of the $Sp\bar{p}S$ accelerator, the pp and the $p\bar{p}$ elastic scattering data were measured at the same $\sqrt{s} = 31, 53$ and 62 GeV.

in the low $|t|$ region. In Ref. [9] the parametrization was shown to be applicable to proton-antiproton scattering as well. Its connection with inelastic reactions is discussed on p. 185 of Ref. [10].

The PB ansatz reads

$$\mathcal{A}(s, t) = i[\sqrt{A} \exp(Bt/2) + \exp(i\phi(s))\sqrt{C} \exp(Dt/2)], \quad (1)$$

where s and t are the standard Mandelstam variables; A, B, C, D , and ϕ were fitted to each energy independently; i.e., energy dependence in the PB ansatz enters parametrically.

The success of the simple PB parametrization motivates its further improvement, extension, and utilization. In papers [5, 6] the low- $|t|$ behavior of the PB ansatz was improved by modifying its simple exponential behavior by (a) inclusion of a two-pion threshold required by analyticity and (b) by means of a multiplicative factor reflecting the proton form factor. Achieving good fits to the TOTEM data [4], at the LHC energies of $\sqrt{s} = 7$ TeV, the modified ansatz was used to predict the behavior of the observables at future energies as well as the expected asymptotic behavior of the cross sections.

The model was also tested in [7, 9] against the TOTEM data [4], and, contrary to many alternative models, it works reasonably well. In Ref. [6] the PB ansatz Eq. (1) was improved; in particular, its small- t behavior was modified. The fitted parameters are collected in Table II of that paper. For example, the authors of [6] quote the following values for these parameters for pp scattering at $\sqrt{s} = 53$ GeV: $\sqrt{A} = 6.55$, $\sqrt{C} = 0.034$ in $\sqrt{\text{mb}/\text{GeV}^2}$ and $B = 10.20$, $D = 1.7$ in GeV^{-2} , $\phi = 2.53$ rad.

As already mentioned, in addition to elastic pp scattering, the PB ansatz also describes $p\bar{p}$ data, with a different set of the parameters (see below), thus opening the way to be used as a tool in extracting the Odderon from the difference of the two. However, in its original form, the PB ansatz does not describe the \sqrt{s} dependence of the model parameters.

In this paper, we try to remedy this limitation by combining the appealingly simple and efficient form of its t dependence with energy dependence inspired by the Regge pole model. Work in this direction was started in papers [5–7, 9, 11].

We address the following issues: (1) we smoothly interpolate between the values of the parameters fitted at fixed energy values, (2) extract the Odderon contribution from the difference of the $\bar{p}p$ and pp cross sections, and (3) compare the energy dependence of this difference with the prediction [12] based on perturbative quantum chromodynamics, by which the intercept of the Odderon trajectory equal to one.

The structure of this paper is as follows: in the next section, we introduce the \sqrt{s} dependence of the parameters of the PB model, which in the next section are determined from the fits to data. Then we discuss the results, in particular the \sqrt{s} dependence of the results, including, for example, the Odderon contribution and the Odderon/Pomeron ratio. Finally, we summarize and conclude.

II. THE GENERALIZED PB MODEL

We use the norm where

$$\sigma_{tot} = 4\pi\Im A(t=0) = 4\pi[\sqrt{A} + \sqrt{C} \cos \phi] \quad (2)$$

and

$$\frac{d\sigma}{dt} = \pi|\mathcal{A}(t)|^2 = \pi[Ae^{Bt} + Ce^{Dt} + 2\sqrt{A}\sqrt{C}e^{(B+D)t/2} \cos \phi]. \quad (3)$$

Following the Regge pole theory, we make the following assignment,

$$\sqrt{A} \rightarrow \sqrt{A(s)} = a_1 s^{-\epsilon_{a_1}} + a_2 s^{\epsilon_{a_2}}, \quad \sqrt{C} \rightarrow \sqrt{C(s)} = c s^{\epsilon_c} \quad (4)$$

inspired by the Donnachie and Landshoff model [14] of cross sections [see Eq. (2)] with effective falling (subleading Reggeons) and rising (Pomeron) components. It follows from our fits that the falling (subleading Reggeon) components in \sqrt{C} are small; hence, they are neglected.

The slopes B and D in the Regge pole theory are unambiguously logarithmic in s , providing shrinkage of the cone:

$$B \rightarrow B(s) = b_0 + b_1 \ln(s/s_0), \quad D \rightarrow D(s) = d_0 + d_1 \ln(s/s_0). \quad (5)$$

In the above formulae a normalization factor $s_0 = 1 \text{ GeV}^2$ is implied.

The phase ϕ is the weakest point of this “toy” model or generalized PB model. In Regge theory, it should depend on t rather than on s . Fortunately, at high \sqrt{s} the dependence of ϕ on energy is weak (see the fits below). However, this is not the case as the energy decreases. The best we can do is to fit the data with

$$\cos(\phi(s)) = k_0 + k_1 s^{-\epsilon_{\cos}}. \quad (6)$$

The “low”-energy behavior is a weak point in any case. Apart from the varying phase, we must account in some way for the subleading (f and ω) Reggeon contributions. This is done partly by the inclusion in $\sqrt{A(s)}$ of a decreasing term (absent in \sqrt{C}). A complete treatment of these terms with proper t -dependent signatures will require a radical revision of the model, and we hope to come back to this issue in the future.

Now we proceed with this simple approach that has a chance to be viable at high energies, where the Pomeron and Odderon dominate [13] and the above complications may be insignificant.

To understand better the existence of any connection between the ansatz (1) and the Regge pole model, we plot the values of the parameters A, B, C, D , and ϕ against s and fit their “experimental” values to Regge-like formulas.

This can be done in two complementary ways: A successive “two-step” fit. First, we acquire the values of the parameters A, B, C, D, ϕ from the fits to the pp and $\bar{p}p$ data, then we fit their Regge forms (see below) to the obtained “experimental” values of A, B, C, D, ϕ .

Alternatively, one may determine the parameters of Eqs. (4) and (5) from a single simultaneous fit to all available data. We chose the first option (5 parameters) since otherwise there were too many (at least 12) free parameters. Thus, we proceed with a two-step fit, by which the final values are determined from a fit to the “experimental” values of A, B, C, D , and ϕ .

We fitted separately pp and $p\bar{p}$ in two variables, s and t , by using pp and $p\bar{p}$ data on total and differential cross sections ranging from the ISR to the LHC for pp and from $Spp\bar{S}$ to the Tevatron for $p\bar{p}$.

Here the following remarks are in order:

(1) It is clear from Eqs. (4) and (5) that, while the parameters A and C are particularly sensitive to the data on total cross sections, B and D are correlated mainly with the differential cross sections (the slopes).

(2) Although we are interested mainly in the high-energy behavior (the Odderon), low-energy effects cannot be fully neglected. They are taken into account approximately by including in A and C subleading terms of the type s^ϵ , $\epsilon \approx 0.5$.

(3) Having fitted A, B, C, D , and ϕ , we perform a cross-check by calculating the resulting total cross sections.

(4) At high energies, the proton-proton and antiproton-proton total cross sections are supposed to converge. (We consider only this simple option, although we are aware of alternatives.) Since the existing data are not yet in this asymptotic domain, we introduce an extra constraint.

(5) The most delicate issue is the phase, which in Regge phenomenology is expected to be t , rather than s , dependent. Our fits (and those of [5–7]) show considerable energy dependence of the phase at low energies but weak dependence at high energies, where we are particularly interested in looking for the Odderon signal. Postponing the introduction of a true Regge-pole-motivated, t -dependent phase to a further study, here we assume a simple parametrization $\cos \phi = k_0 + k_1 s^{\epsilon_\phi}$.

III. FITTING THE MODEL TO THE DATA

We have calculated the s dependence of the parameters using a fitting strategy consisting of three consecutive steps described in detail below. In doing so, the following criteria were

applied:

- best χ^2 for each fit;
- the $-t$ range was set within 0.35-2.5 GeV²;
- for each fixed energy, the model was fitted simultaneously to $d\sigma/dt$ and σ_{tot} (focusing on the dip region);
- from the resulting fits, σ_{tot} was reconstructed in the whole available energy range.

The values of the fitted parameters, in general, are consistent, within about 30%, with those obtained in Refs. [3, 6], except for the small value of \sqrt{C} deviating considerably from those quoted in the above papers, which used a different t range for their data analysis.

Energy (GeV)	\sqrt{A}	B	\sqrt{C}	D	$\cos(\phi)$	χ^2/NDF
23.4	$3.13 \pm 0.6\%$	$8.66 \pm 0.4\%$	$0.019 \pm 8.3\%$	$1.54 \pm 5.1\%$	$-0.97 \pm 0.3\%$	1.6
30.5	$3.21 \pm 0.2\%$	$8.95 \pm 0.3\%$	$0.014 \pm 7.4\%$	$1.28 \pm 5.6\%$	$-0.98 \pm 0.2\%$	1.1
44.6	$3.33 \pm 0.7\%$	$9.32 \pm 0.5\%$	$0.017 \pm 8.0\%$	$1.45 \pm 5.3\%$	$-0.93 \pm 0.8\%$	1.7
52.8	$3.38 \pm 0.3\%$	$9.44 \pm 0.6\%$	$0.017 \pm 7.6\%$	$1.43 \pm 5.0\%$	$-0.92 \pm 0.9\%$	1.1
62.0	$3.49 \pm 0.5\%$	$9.66 \pm 0.6\%$	$0.018 \pm 9.9\%$	$1.53 \pm 6.3\%$	$-0.92 \pm 1.6\%$	1.5
7000.0	$8.51 \pm 1.6\%$	$15.05 \pm 0.8\%$	$0.670 \pm 2.3\%$	$4.71 \pm 0.8\%$	$-0.93 \pm 0.3\%$	1.4

TABLE I. Values of the parameters from a fit to the pp data at various \sqrt{s} . The quoted errors correspond to the relative errors, as given by CERN MINUIT fitting package (status= converged, error matrix accurate).

A. Step 1: Fitting the parameters A, B, \dots to $d\sigma/dt$ and σ_{tot} for fixed energies

Figure 2 shows a fit to the data on the pp and $\bar{p}p$ differential and total cross sections. The parameters A, B, C, D , and ϕ were fitted to each energy separately. Given the simplicity of the model, the fits look reasonable.

Figure 3 shows the fitted values of the parameters A, B, C, D , and ϕ both for pp and $\bar{p}p$ scattering to be used as “experimental” data in the second stage of our fitting procedure, in which the explicit expressions (4), (5) and (6) are inserted. The fitted values of the parameters and relevant χ^2/NDF values are quoted in Tables I and II.

Note the difference between the present model and that of Refs. [5–7] in the low- $|t|$ behavior of the differential cross section, corrected in [5–8] and taking account of the deviation from an exponential. Normalization in Ref. [3] is arbitrary since, in that paper, only the differential cross section is shown. Total cross sections are not shown in the above papers.

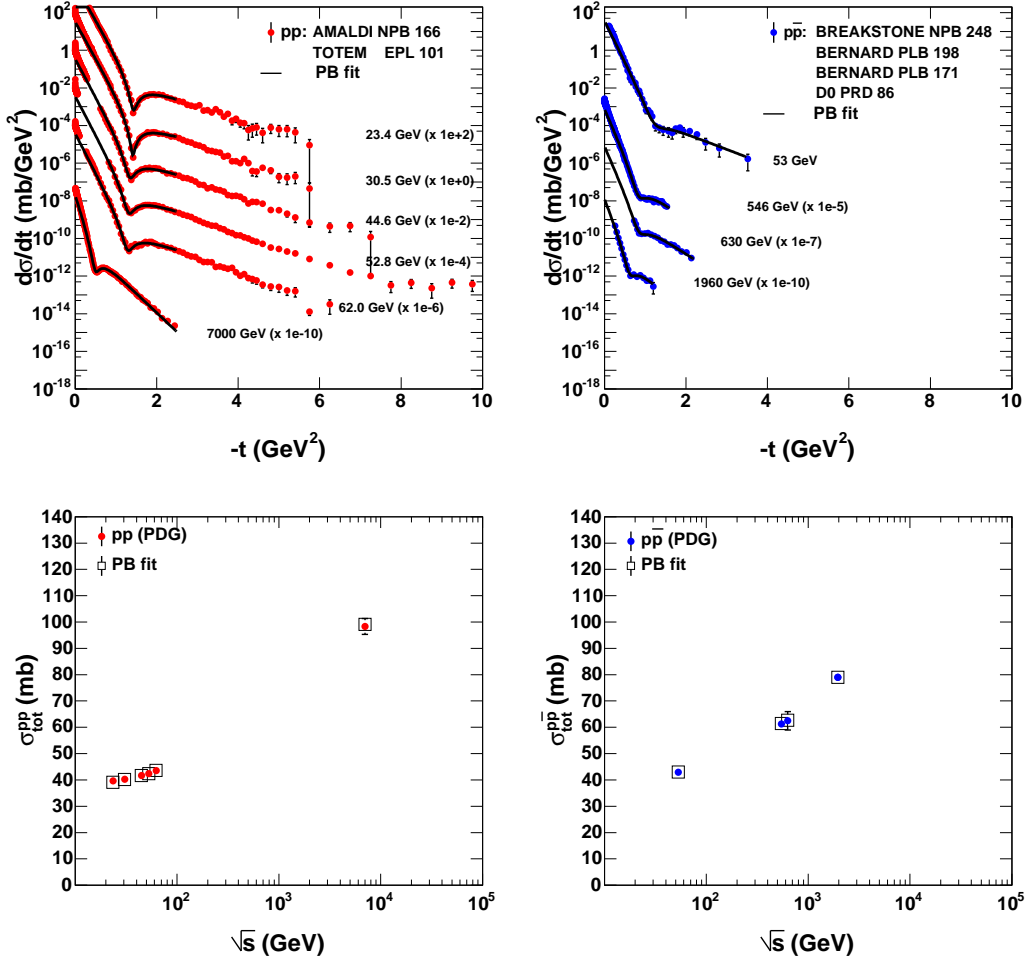


FIG. 2. The PB model fitted to the pp and $\bar{p}p$ data at discrete energy values. The $d\sigma/dt$ data are from Refs. [16–21]. The data on σ_{tot} are from the Particle Data Group database [22].

Energy (GeV)	\sqrt{A}	B	\sqrt{C}	D	$\cos(\phi)$	χ^2/NDF
63	$3.43 \pm 1.1\%$	$10.07 \pm 1.3\%$	$0.022 \pm 30.8\%$	$1.90 \pm 14.8\%$	$-0.60 \pm 22.7\%$	0.7
546	$5.06 \pm 1.2\%$	$11.25 \pm 1.3\%$	$0.204 \pm 21.0\%$	$3.55 \pm 8.6\%$	$-0.86 \pm 2.7\%$	0.6
630	$5.13 \pm 3.9\%$	$11.26 \pm 3.7\%$	$0.176 \pm 26.6\%$	$3.23 \pm 9.6\%$	$-0.81 \pm 7.9\%$	0.5
1960	$6.85 \pm 3.7\%$	$12.46 \pm 3.3\%$	$0.629 \pm 41.6\%$	$4.69 \pm 15.4\%$	$-0.90 \pm 3.6\%$	0.4

TABLE II. Values of the parameters fitted to $\bar{p}p$ data

B. Step 2: Fitting the parameters a_i, b_i, \dots entering Eqs. (4), (5) and (6) to the “data” $A, B, C, D, \cos(\phi)\dots$, quoted in Tables I and II.

The resulting values of the parameters after the second stage of fitting are

$$\begin{aligned}
 \sqrt{A_{pp}(s)} &= 1.31s^{0.106} + 3.90s^{-0.298}, \\
 \sqrt{C_{pp}(s)} &= 0.00117s^{0.358}, \\
 B_{pp}(s) &= 5.13 + 0.555 \ln s, \\
 D_{pp}(s) &= -0.838 + 0.312 \ln s. \\
 \cos(\phi_{pp}(s)) &= -0.928 - 0.863s^{-0.429}.
 \end{aligned} \tag{7}$$

$$\begin{aligned}
 \sqrt{A_{p\bar{p}}(s)} &= 1.31s^{0.106} + 4.28s^{-0.298}, \\
 \sqrt{C_{p\bar{p}}(s)} &= 0.00177s^{0.358}, \\
 B_{p\bar{p}}(s) &= 7.87 + 0.274 \ln s, \\
 D_{p\bar{p}}(s) &= -0.552 + 0.312 \ln s, \\
 \cos(\phi_{p\bar{p}}(s)) &= -0.928 + 4.37s^{-0.328}.
 \end{aligned}$$

The lowest right icon in Fig. 3 is a “cross-check”, showing the pp and $\bar{p}p$ total cross sections calculated from Eq. (2) with the explicit values of the parameters defined by (4), (5) and (6). The $\bar{p}p$ total cross section turns down at highest energies, deflecting dramatically from that of pp . The reason for that nonphysical effect is the scarcity of $p\bar{p}$ data, leaving too much freedom in the high-energy extrapolation of the cross section, where one expects asymptotic equality $\sigma_t^{p\bar{p}} = \sigma_t^{pp}$ for $s \rightarrow \infty$; see Eq. (47) in Ref. [15]. This deficiency should, and can, be cured by imposing an additional constraint on the model. This will be done in the next subsection, by fixing (tuning) the parameter ϵ_{a_2} (the leading powers in s of \sqrt{A}) to be the same in pp and $\bar{p}p$ scattering.

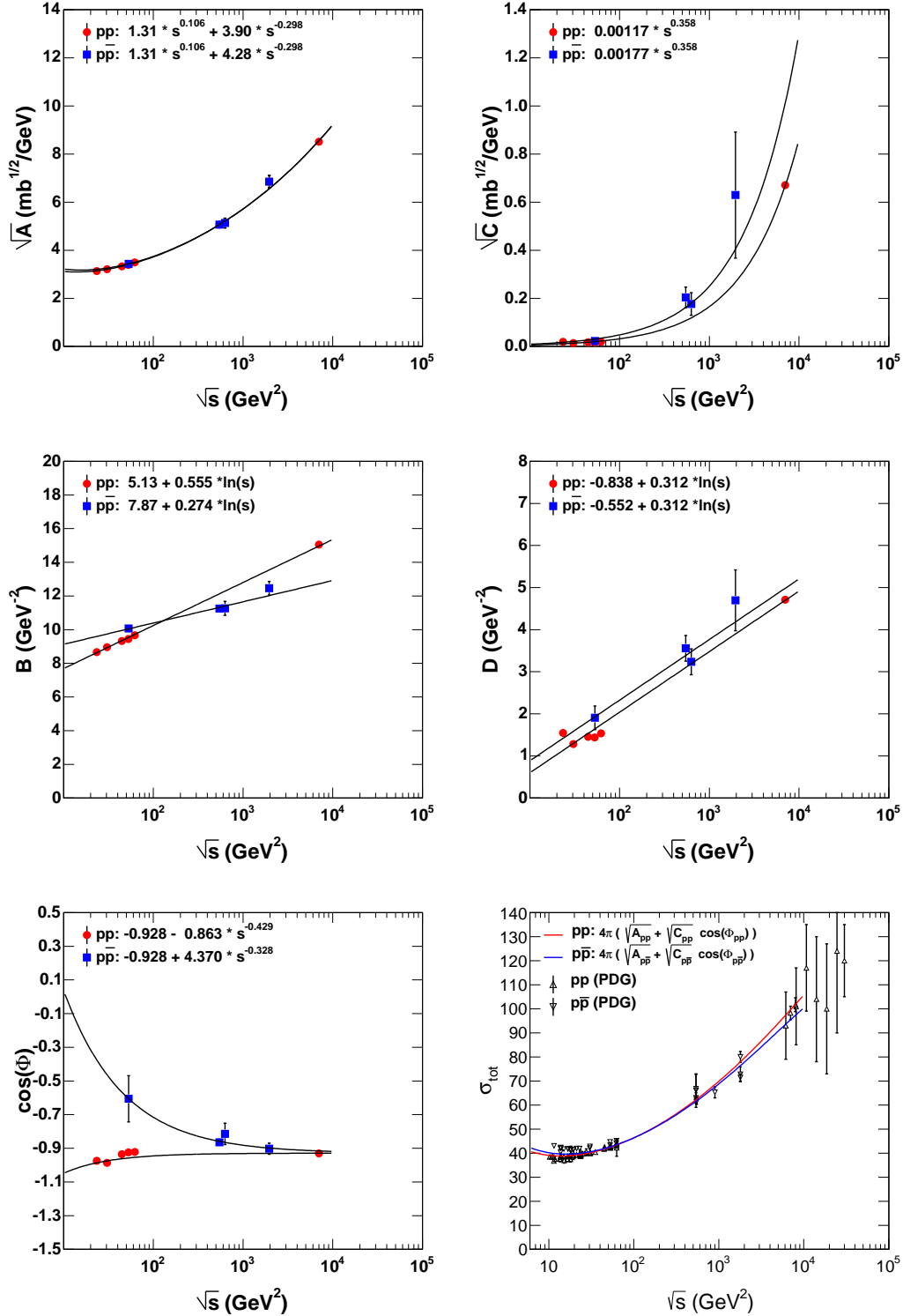


FIG. 3. Energy-dependent values of the parameters extracted from a fit to pp and $p\bar{p}$ data. The data on σ_{tot} are from the Particle Data Group database [22].

C. Step 3: Tuning (refitting) the parameters by imposing the asymptotic constraint $\sigma_t^{p\bar{p}} = \sigma_t^{pp}$, $s \rightarrow \infty$

The above, unbiased fit does not satisfy automatically the required (see [15]) asymptotic constraint $\sigma_t^{pp} = \sigma_t^{p\bar{p}}$ since the available freedom (especially due to the lack of simultaneous pp and $p\bar{p}$ elastic scattering data at $\sqrt{s} = 540, 630, 1800$ and 7000 GeV) leaves much freedom for the extrapolation to energies beyond the existing accelerators. To remedy this problem, we have tuned the parameters to meet the above constraint in the currently available energy range. Below are the results of the “tuned” fit (see Fig. 4) satisfying the asymptotic condition $\sigma_t^{pp} = \sigma_t^{p\bar{p}}$ in the $\sqrt{s} \leq 14$ TeV energy range.

The refitted s -dependent values of the parameters for pp and $p\bar{p}$ scatterings are

$$\begin{aligned}
 \sqrt{A_{pp}(s)} &= 1.41s^{0.0966} + 2.78s^{-0.267}, \\
 \sqrt{C_{pp}(s)} &= 0.00223s^{0.308}, \\
 B_{pp}(s) &= 4.86 + 0.586 \ln s, \\
 D_{pp}(s) &= -0.189 + 0.250 \ln s. \\
 \cos(\phi_{pp}(s)) &= -0.928 - 0.838s^{-0.425}.
 \end{aligned} \tag{8}$$

$$\begin{aligned}
 \sqrt{A_{p\bar{p}}(s)} &= 1.41s^{0.0996} + 4.00s^{-0.267}, \\
 \sqrt{C_{p\bar{p}}(s)} &= 0.00588s^{0.264}, \\
 B_{p\bar{p}}(s) &= 6.55 + 0.398 \ln s, \\
 D_{p\bar{p}}(s) &= 2.351 + 0.068 \ln s, \\
 \cos(\phi_{p\bar{p}}(s)) &= -0.908 + 4.376s^{-0.328}.
 \end{aligned}$$

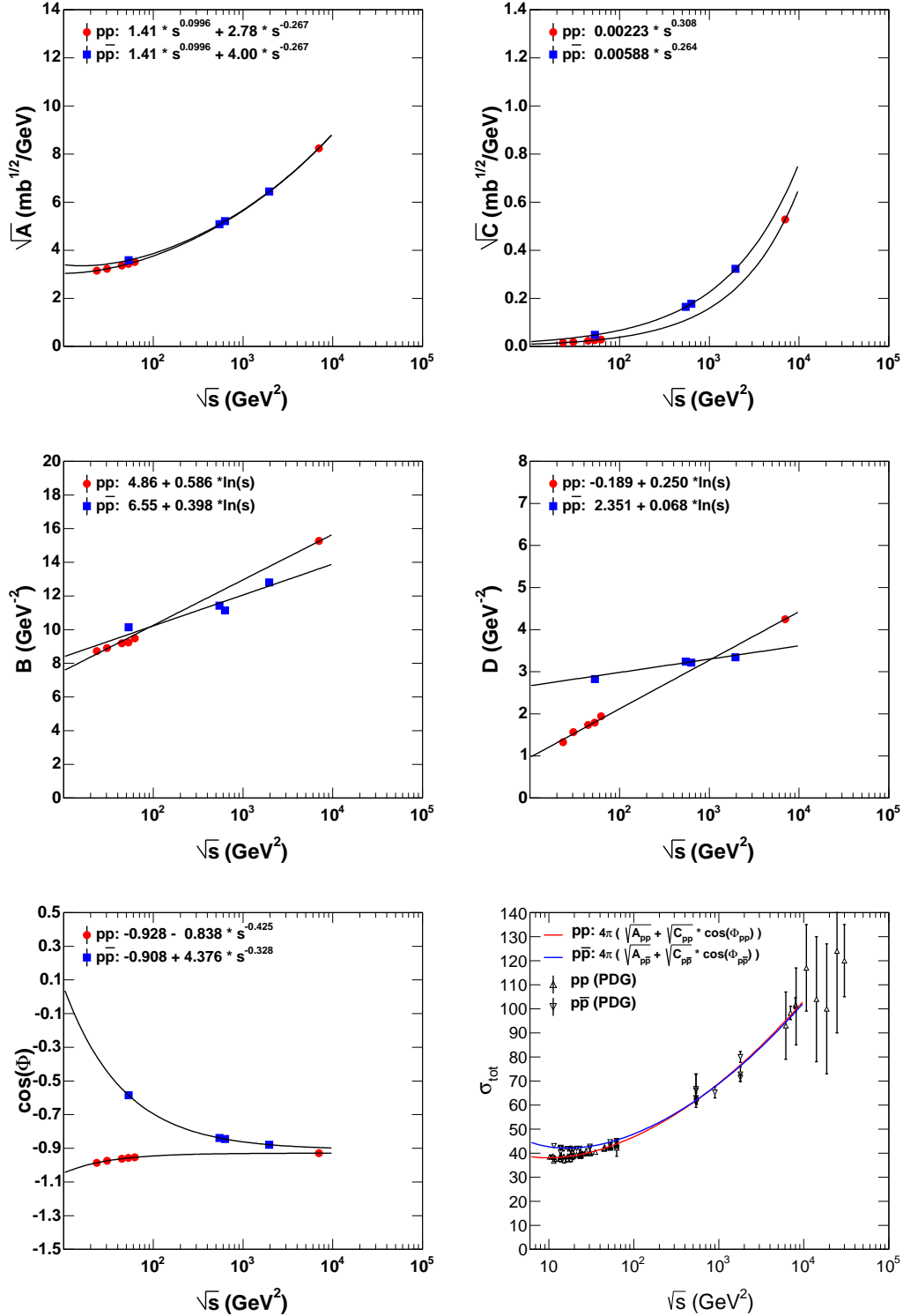


FIG. 4. Energy-dependent values of the parameters from a fit to pp and $p\bar{p}$ data, constrained by $\sigma_t^{p\bar{p}} = \sigma_t^{pp}$ as $\sqrt{s} \rightarrow \infty$. The lowest right icon shows a cross-check for the (asymptotically converting) total cross sections.

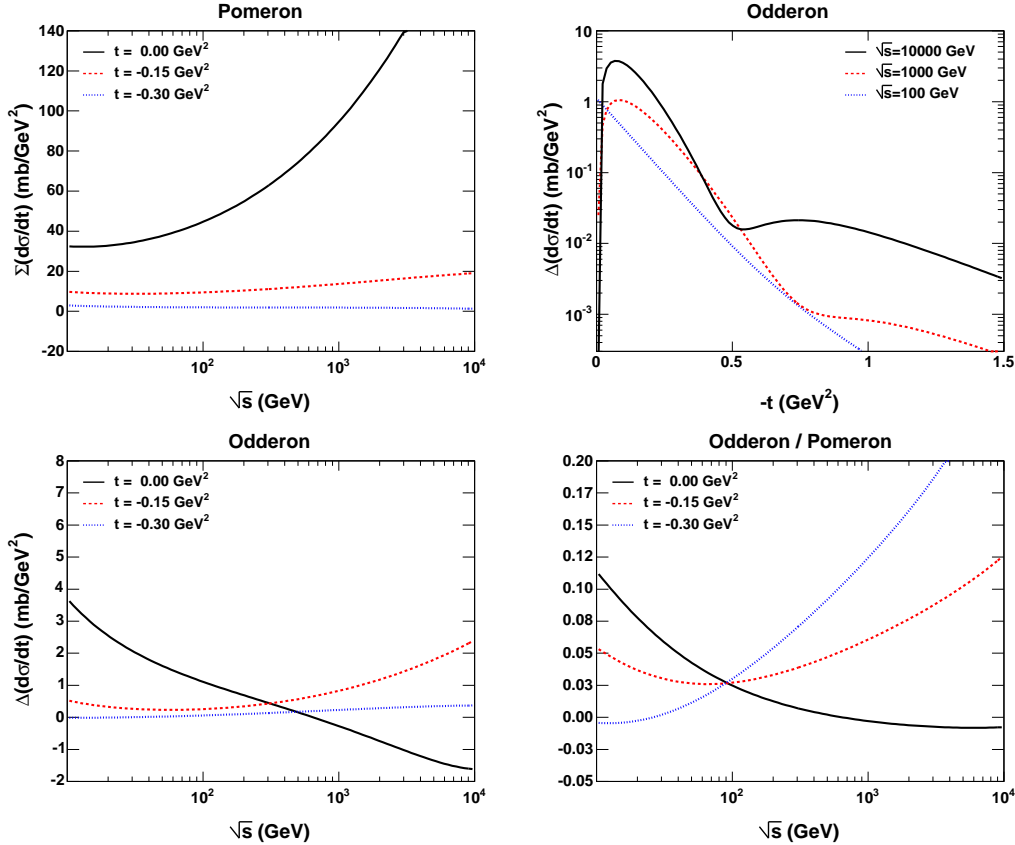


FIG. 5. Odd (Odderon) and even (Pomeron) parts of the $d\sigma/dt$ cross sections calculated from the difference $|\mathcal{A}_{\bar{p}p}^2 - |\mathcal{A}_{pp}^2 = \Delta_{Odd}$ and from the sum $|\mathcal{A}_{\bar{p}p}^2 + |\mathcal{A}_{pp}^2 = \Sigma_{Pom}$ fitted to the data.

IV. THE ODDERON

The existence of a parametrization for both pp and $\bar{p}p$ scattering offers the possibility to extract the odd- C contribution by using the formula

$$\mathcal{A}_{\bar{p}p} = \mathcal{A}_{even} \pm \mathcal{A}_{odd}, \quad (9)$$

where \mathcal{A}_{even} and \mathcal{A}_{odd} are, respectively, the C -even and C -odd components of the scattering amplitude; see Table 1 in Ref. [13].

While the C -even component contains the Pomeron and the f trajectory (both known), the C -odd part is made of the poorly known Odderon and the familiar ω trajectory. At the LHC energies, the contribution from secondary trajectories, e.g., f and ω , is negligible (see Ref. [13]); therefore, by taking the difference between the known (fitted) $p\bar{p}$ and pp amplitudes, one gets a pure odd- C contribution that, in the LHC energy range, is the Odd-

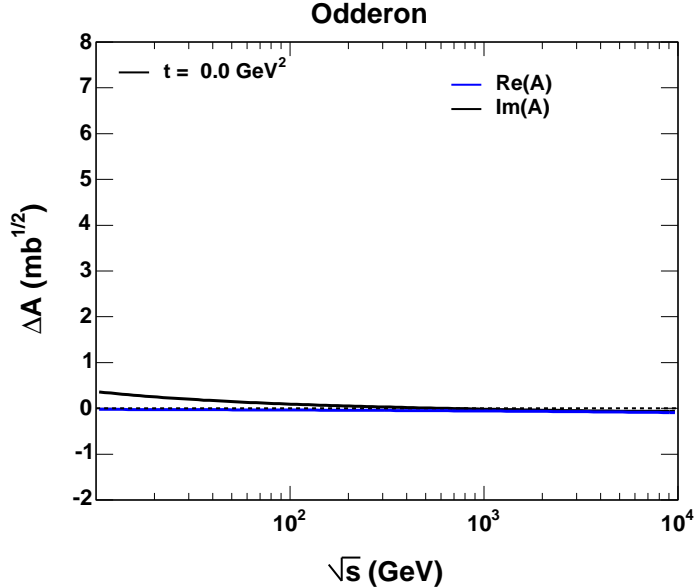


FIG. 6. Real and imaginary parts of the difference $\mathcal{A}^{\bar{p}p} - \mathcal{A}^{pp} = \Delta\mathcal{A}$ calculated from the present model fitted to the data. As seen from the figure, this difference tends to a (small) constant, corresponding to a unit intercept Odderon [12].

eron. From the explicit expressions for pp and $\bar{p}p$ amplitudes (cross sections), we calculate the Odderon amplitude (or its contribution to the cross section) by taking the difference $\mathcal{A}^{\bar{p}p} - \mathcal{A}^{pp} = \mathcal{A}_{Odd}$. The result (the energy dependence for several fixed values of t and t dependence for several fixed values of s) is shown in Fig. 4.

The extracted model parameters are used then to evaluate the even and odd contributions to the forward scattering amplitude. In Fig. 5 we show the Pomeron and the Odderon contributions as the sum or the difference of the differential cross section of $p\bar{p}$ and pp elastic scattering. We see that, as expected, the Pomeron dominates at large colliding energies, while the Odderon contribution is small and at $t = 0$ even changes sign. A particularly interesting feature is shown on the lower right panel of Fig. 5, where the Odderon/Pomeron ratio is shown at different values of t at various \sqrt{s} . Apparently, at $\sqrt{s} \approx 100$ GeV, the Odderon/Pomeron ratio becomes t independent and the t -dependent curves pass through the same point of about 0.03.

An important finding of our paper is the near energy independence of the odd- C contribution to the scattering amplitude, which, at high (e.g., those of the LHC) energies, is dominated by the Odderon exchange. In Fig. 6 we plot the odd- C contribution calculated

from the difference (9). Both the real and imaginary parts of this difference at $t = 0$ tend to a (small) constant value, which correspond to a unit-intercept Odderon as predicted [12] from quantum chromodynamics.

V. CONCLUSIONS

The present work is a semiquantitative estimate of the possible odd- C contribution to the scattering amplitude (cross sections) at high energies. “Semiquantitative” implies limitations due to the following:

- For the sake of simplicity, we ignore the low- t nonexponential behavior (sharpening) of the differential cross section. This simplification has dramatic impact on the low- t behavior of the Odderon contribution because of the large errors due to the cancellation of the Pomeron contribution. The importance of the low- t effects was emphasized, e.g., in Refs. [5, 6].
- The s - (rather than t -) dependent signature factor (phase) is in agreement with the data, but it is in contrast to expectations based on Regge phenomenology.
- The odd- C contribution to the amplitude, equal to the difference (9), shown in Fig. 6, tends to a constant limit determined by a unit-intercept Odderon, predicted by Bartels, Lipatov, and Vacca [12].
- It is an oversimplified treatment of the low-energy (“secondary Reggeons”) contributions (Odderon and Pomeron here implies, generally, odd and even exchanges).
- There is the absence, for the moment, of any physical interpretation in terms of Reggeon exchanges of the components in the PB ansatz.

Given these limitations and simplifications, our approach can be considered as semiquantitative, showing however some new aspects of the enigmatic Odderon.

We strongly recommend to run the LHC accelerator at the injection energy $\sqrt{s} = 900$ GeV and at the Tevatron energy of 1.8-1.96 TeV, so that the missing energy range of pp elastic scattering will be covered and elastic pp scattering data will be measured in the region where elastic $p\bar{p}$ scattering is already measured. It would also be desirable to measure elastic pp scattering at the $\sqrt{s} = 500$ GeV region — the upper energy range of the RHIC accelerator.

Using the presently available data, the indefinite rise of the $C(s)$, multiplied by a negative “signature factor” $\cos \phi$, prevents the use of the generalized PB model beyond the LHC energy region.

In the future we intend to

- rewrite the PB ansatz with correct, t -dependent Regge signature factors [11], remembering that in the present study the even and odd parts of the amplitude differ only by the values of the fitted parameters, without the identification of particular Regge exchanges (trajectories);
- fit to the data to provide hints concerning the physical meaning of the components (two or more); for example, our fits (and those of Refs. [3, 5–7]) indicate that $A \gg C$, but C rises with energy faster than A . Similar considerations may help in relating the second term with the Odderon or a “hard” Pomeron, for which the slopes (B and D) may be indicative.
- add lower-lying contributions (subleading Reggeons) which are inevitable at lower energies, at the price of giving up of the attractive simplicity of the model;
- use other asymptotic Pomernanchuk-like constraints in determining the parameters (see the work in Ref. [8] that points to this interesting direction);
- calculate and fit the model to other observables, e.g., the ratio of the real to imaginary parts of the amplitude $\rho(s, t)$, of the slope $B(s, t)$, etc. Its relation to inelastic processes (see [10]) may offer additional information.

ACKNOWLEDGMENTS

L.J. acknowledges cordial hospitality by the Wigner RCP, Budapest, Hungary, where this work was completed. He is also grateful to D.A. Fagundes and G. Pancheri for useful discussions and correspondence. This work was partially supported by the Hungarian OTKA

- [1] L.L. Jenkovszky and B.V. Struminsky, Report No. ITP-88-170 Preprint, Kiev, 1988;
A. P. Contogouris, L. L. Jenkovszky, E. Martynov, and B. Struminsky, *Phys. Lett. B* **298**, 432 (1993);
V. P. Goncalves, *Nucl. Phys.* **A902**, 32 (2013).
- [2] C. Ewerz, M. Maniatis, and O. Nachtmann, *Ann. Phys. (Amsterdam)* **342**, 31 (2014).
- [3] R. J. N. Phillips and V. D. Barger, *Phys. Lett.* **46B**, 412 (1973).
- [4] G. Antchev *et al.* (TOTEM Collaboration), *Europhys. Lett.* **95**, 41001 (2011).
- [5] A. Grau, S. Pacetti, G. Pancheri, and Y. N. Srivastava, *Phys. Lett. B* **714**, 70 (2012).
- [6] D. A. Fagundes, A. Grau, S. Pacetti, G. Pancheri, and Y. N. Srivastava, *Phys. Rev. D* **88**, 094019 (2013).
- [7] D. A. Fagundes, A. Grau, S. Pacetti, G. Pancheri, and Y. N. Srivastava, *Proc. Sci, DIS* (2013) 306.
- [8] G. Pancheri, D. A. Fagundes, A. Grau, and Y. N. Srivastava, *Nuovo Cimento Soc. Ital. Fis.* **037**, 179 (2014).
- [9] L. Jenkovszky and D. Lontkovskiy, Lessons from the first measurements of elastic pp scattering at the LHC, in *New Trends in High-Energy Physics*, edited by P.N. Bogolubov and L.L. Jenkovszky (L. L., Kiev, 2011), p. 305, Bogolyubov Institute for Theor. Physics, Nat. Ac. Sc. of Ukraine, <http://crimea.bitp.kiev.ua/crimea2011/>; L. Jenkovszky and D. Lontkovskiy, in *Proc. of Rencontres du Vietnam, 14th Workshop on EDS 2011*, SLAC eConf C111215, edited by Mary Ann Rotondo and Chung I-Tan, Stanford National Accelerator Laboratory.
- [10] K. A. Goulianos, *Phys. Rep.* **101**, 169 (1983).
- [11] L. Jenkovszky, *Nuovo Cimento Soc. Ital. Fis.* **037**, 99 (2014).
- [12] J. Bartels, L.N. Lipatov, and G.P. Vacca, DESY arXiv:hep-ph/9912423.
- [13] L. L. Jenkovszky, A. I. Lengyel, and D. I. Lontkovskiy, *Int. J. Mod. Phys. A* **26**, 4755 (2011).
- [14] A. Donnachie and P. V. Landshoff, *Nucl. Phys.* **B231**, 189 (1984).
- [15] A. N. Wall, L. L. Jenkovszky, and B. V. Struminsky, *Fiz. Elem. Chastits At. Yadra* **19**, 180 (1988).
- [16] U. Amaldi and K. R. Schubert, *Nucl. Phys.* **B166**, 301 (1980).

- [17] G. Antchev *et al.* (TOTEM Collaboration), *Europhys. Lett.* **101**, 21002 (2013).
- [18] A. Breakstone *et al.* (AMES-BOLOGNA-CERN-DORTMUND-HEIDELBERG-WARSAW COLLABORATION), *Nucl.Phys.* **B248**, 253 (1984).
- [19] D. Bernard *et al.* (A4 Collaboration), *Phys. Lett. B* **198**, 583 (1987).
- [20] D. Bernard *et al.* (UA4 Collaboration), *Phys. Lett. B* **171**, 142 (1986).
- [21] V. M. Abazov *et al.* (D0 Collaboration), *Phys. Rev. D* **86**, 012009 (2012).
- [22] J. Beringer *et al.* (Particle Data Group Collaboration), *Phys. Rev. D* **86**, 010001 (2012).